

UAV Coverage Using Hexagonal Tessellation*

Esra Kadioglu¹, Cetin Urtis² and Nikolaos Papanikolopoulos³

Abstract—Unmanned aerial vehicles (UAVs) are increasingly being used for coverage applications. Some common examples include inspecting agricultural fields for certain plant diseases, tracking wildfire, photogrammetry, flying over an area to find avalanche victims, and several other search and rescue operations. Although fixed-wing UAVs can survey large areas more quickly and have a better battery lifetime compared to multirotor systems, they fail to provide a close up inspection of a certain area by hovering over it. Quadrotors provide excellent inspection capabilities; however, they have notoriously short battery lifetimes. In this paper, we propose a coverage algorithm through hexagonal tiling of a target region. We present a coverage path using the average distance, d , that can be travelled by a drone on a single charge, and the radius, r , of the viewing cone of a typical downward facing camera mounted on it as parameters. We compare our method with classical zigzag coverage pattern. Our results show that for large enough regions, the Hamiltonian circuit that passes through the centers of the tiling hexagons produces a shorter path.

I. INTRODUCTION

Coverage Path Planning (CPP) is the problem of finding a path that covers the entire region of interest. This process involves two stages: Area decomposition into cells and path planning among the cells. The problem has been widely studied for ground robots [1] and it has found new challenges [2], [3] with the widespread use of UAVs in applications such as surveillance [4], [5], search and rescue [6], [7], and agriculture [8], [9].

Comprehensive surveys on coverage path planning algorithms are given in [1], [2], and [3]. Cabreira et al. addresses specifically the case of UAVs in [3]. They give an extensive survey of coverage algorithms and their performances in [3] such as back-and-forth motion (zigzag), spiral, sector search, barrier patrol, energy aware spiral (where the UAV performs wider turns), Hilbert curves, gradient based, wavefront algorithm, harmony search etc. To the best of our knowledge, our proposed method of hexagon tessellation of a region and the resulting coverage path by Hamiltonian circuit is not mentioned.

The coverage problem has been addressed by several authors from a geometric point of view, however, the energy

limitations of the robot places additional constraints. Efficient coverage paths are particularly important for UAVs since the robots can fly only for a short time. This can be achieved in a number of ways such as devising shorter paths, using heuristic approaches, reducing the number of turns, covering only select target areas instead of the entire region, etc. In [10] an algorithm is proposed to solve the multi-robot persistent coverage problem which is expressed as a variant of the vehicle routing problem (VRP). The VRP is NP-hard, therefore a heuristic method is presented to compute bounded suboptimal results in real time. In this work, a team of robots with a specified fuel capacity efficiently cover a given set of targets persistently over long periods of time. The problem is expressed as a mixed integer linear program formulation and a Hamiltonian path through target points is computed.

Di Franco and Buttazzo perform image reconstruction by photogrammetry by decomposing the area of interest into rectangles and programming a trajectory through their centers [11]. This is similar to our work; however, a rectangular tiling is applied and a sweeping motion is used for the path. The number of turns on the sweeping path affects the time of completion since the robots need to decelerate, turn, and accelerate. So the authors optimize the path by setting the scan direction parallel to the longest bounding line on the region. Two classical coverage algorithms, spiral and zigzag motion are compared in [12] where the authors modify the algorithms with respect to a UAV energy model developed in [13]. In this paper, it is shown that the spiral algorithm outperforms the zigzag, however, there is a varying degree of overlap in captured images and the overall path do not take return to launch into account, i.e. the UAV returns to its starting location in the end by following a straight line path.

Wei and Isler also work on an energy efficient coverage algorithm in [14]. A given polygon is partitioned into contour connected pieces. The robot follows the contours and when the remaining energy is just enough for going back to the charging station, it retreats. The strategy essentially performs a depth-first-search-like coverage.

In [15] a known area with obstacles is first divided into cells using boustrophedon cell decomposition and then an Eulerian circuit is generated as the coverage path using integer linear programming. The coverage direction is important since it can affect the number of sweep lines and turns. As such, different strategies are presented for selecting the direction of coverage. Experiments are performed by using a fixed-wing UAV. A method for minimizing the lines -and therefore the number of turns- in coverage is also presented in [16].

In some applications, there may be specific regions of

*Esra Kadioglu is supported by TUBITAK-BIDEB 2219 postdoctoral research scholarship program.

¹Esra Kadioglu is with Computer Engineering Department, TOBB University of Economics and Technology, Ankara, Turkey. She is currently a visiting researcher at the Center for Distributed Robotics, University of Minnesota. kadio004@umn.edu

²Cetin Urtis is with the Department of Mathematics, TOBB University of Economics and Technology, Ankara, Turkey. He is currently a visiting Fulbright Scholar at the Department of Mathematics, University of Minnesota. urtis002@umn.edu

³Nikolaos Papanikolopoulos is with the Department of Computer Science and Engineering, University of Minnesota. npapas@cs.umn.edu

interest (RoIs). In such cases, a complete coverage is not feasible. In [17], the drone makes an online computation of RoI at a higher altitude and constructs a tree structure to perform coverage of these sub-areas. The approach is compared to the standard lawnmower method and shown to outperform it by a factor of 1.7 in certain cases.

Lim and Bang use a hexagonal grid in [18] but in a different context than ours. In their work, UAVs perform a surveillance mission and information points -representing their surroundings- are located at the vertices of hexagons tiling the area.

In this paper, we use the result that the number of hexagons required to tile a given area is smaller than the number of squares [19]. The size of the tiling polygons is specified using the radius of the viewing cone of the camera mounted on the drone as a parameter. In this way, we can adjust the path with respect to the desired resolution of the images, the specific altitude of the drone, etc. We use a Hamiltonian path that passes through the *centers* of the tiling hexagons to create a coverage path for a drone. The path created takes return to the launch location into account. We establish bounds on the area of the region where the path through a hexagonal tessellation is shorter than a path through a square tessellation. Given the desired resolution, i.e. the radius of the viewing cone, it is possible to compute the size of the area that can be inspected by the drone with a single charge.

II. PROBLEM STATEMENT

A. Preliminaries

We use a rectangular area to perform our tessellation on. A hexagonal and a square tessellation are performed. In each case, the hexagon or the square is enclosed in a circle. This circle represents the viewing cone of the downward facing camera on the UAV. Therefore, the size of the cells are proportional to the footprint of the camera. We modeled our parameters from a DJI Matrice quadrotor equipped with a downward facing camera in our lab. We assume a useful flight time of 20 minutes. At a speed of 1 to 2 meter/s the drone could traverse between 1200 to 2400 meters. The camera has a field of view of approximately 60 degrees. Assuming a height of between 10 and 20 meters above ground level and neglecting any influence of camera distortion, a viewing cone radius would fall between about 6 and 12 meters. We take the cone radius, r as 10 meters.

B. Problem Description

Suppose that we would like to obtain a complete coverage of a given region, R . Coverage is achieved when the viewing cone of the drone camera sweeps the entire region as the drone completes its path (See Figure 1). We assume that the region is two dimensional and there are no obstacles for the drone in the air, i.e. no hills, high-rise buildings etc..

The drone is equipped with a downward facing camera and the region that is within the field of view of the camera is a disc of radius r . The drone starts its path from A and takes a picture each time it is at the center of the circular regions denoted by c_1, c_2, \dots, c_n , and then finishes at A . We



Fig. 1. Drone camera sweeping the region.

would like to find the shortest path that will allow the drone to achieve a complete coverage of the area, R .

If we consider circular regions as images captured by the drone, all points in the area R should be covered. This is a type of the Discrete Unit Disk Cover (DUDC) problem, which is stated as: Given a set P of n points and a set \mathcal{D} of m unit radius disks in the plane, DUDC problem is to find a subset of \mathcal{D} of minimum cardinality covering P . DUDC problem is shown to be NP-complete [20], [21].

There are many known approximation algorithms for DUDC using a variety of techniques. Most of the approximation algorithms for DUDC are theoretical in the sense that they prove the existence of a coverage but they do not consider implementations. Therefore, these are not useful for our purposes. In order to apply a DUDC problem solution to our scenario, the drone will fly through the center of the circles. A solution which has a pattern will be better in providing a smooth flying route for the drone. The theoretical solutions only provide the locations of the center points, however, they do not consider a smooth path traversing these points. For the purposes of UAV flight, such a path is essential. There are approximation algorithms which use square tessellation and hexagonal tessellation in [22], [23], [24].

It is known that in order to cover a sufficiently large area in the plane, unit hexagon tessellation uses less number of polygons than that of unit square tessellation [19].

III. COVERAGE COMPARISON

In this section, we compare the effectiveness of the coverages obtained by square and hexagon tessellations. A tessellation is the process of creating a two-dimensional plane using one or more geometric shapes with no overlaps and no gaps. A regular tessellation is the one that uses regular polygons of the same shape and same size. It is known that there are only three regular tessellations: hexagon, square, and triangle [25].

A regular polygon enclosed by a unit disk is called a unit polygon. When the polygons of a regular tessellation

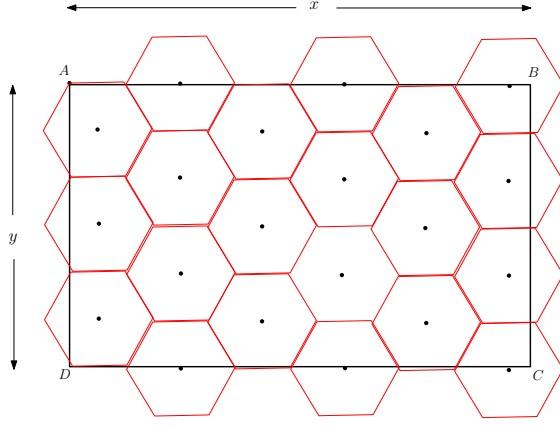


Fig. 2. Hexagonal tessellation of the rectangle $ABCD$. Coinciding the hexagon vertex with A and edge with $[AB]$ provides a unique tessellation.

are all unit polygons, the tessellation is called unit polygon tessellation.

Lemma 1: To cover a sufficiently large region in the plane, the unit hexagon tessellation requires less number of polygons than that of the other two (square and triangle) unit polygon tessellations.

Proof: Suppose that the region R is covered by triangle, square and hexagon tessellations separately. We consider triangles, squares and hexagons which are in those tessellations.

Suppose that the area of the region is F . Dividing the area of the region by the areas of a triangle, a square and a hexagon we get the number of triangles, squares and hexagons approximately as:

$$N_T = \left\lceil \frac{4F}{3\sqrt{3}} \right\rceil, \quad N_S = \left\lceil \frac{F}{2r^2} \right\rceil \quad \text{and} \quad N_H = \left\lceil \frac{2F}{3\sqrt{3}r^2} \right\rceil$$

respectively. ■

Since the number of polygons in the triangle tessellation is twice the number of polygons in the hexagon tessellation, we only consider square and hexagon tessellations. For further analysis, we can give more accurate numbers of polygons in square and hexagon tessellations: Assume that the polygons are enclosed in a disc of radius r . One side of a polygon in square and hexagon tessellations are $r\sqrt{2}$ and r respectively. Since one can cover the region by rectangles we consider the case where the region is a rectangle. Suppose the rectangle is denoted by $ABCD$ and in both tessellations one vertex of the polygon is aligned at A and one edge is on the line AD (see Figure 2 and Figure 6). Also, suppose that $|AB| = x$ and $|AD| = y$. AB corresponds to the major axis and AD corresponds to the minor axis of the rectangle.

The number of squares N_S in the square tessellation can be given as follows:

$$N_S = \left\lceil \frac{x}{r\sqrt{2}} \right\rceil \left\lceil \frac{y}{r\sqrt{2}} \right\rceil$$

Here the first factor gives the number of squares in the direction A to B (i.e. along the long edge of the rectangle, the

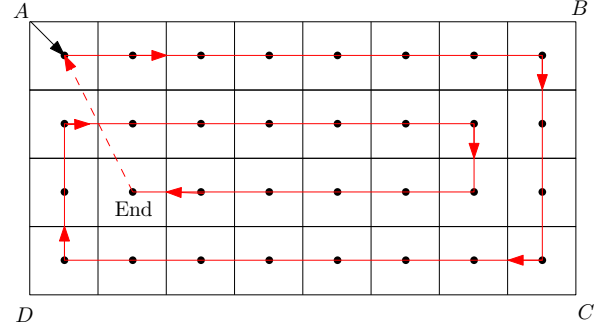


Fig. 3. Coverage by square tessellation with a spiral path. The coverage path that starts and ends at A is shown.

major axis) and the second factor gives the number of squares in the direction A to D (i.e. along the short edge of the rectangle, the minor axis). Also we use the ceiling function to make sure that we count the squares which overflow the rectangle.

Similarly, the number of hexagons N_H in the hexagon tessellation can be given as follows:

$$N_H \leq \lfloor ab \rfloor$$

where

$$a = \left\lceil \frac{2(x - r/2)}{3r} \right\rceil + 1$$

and

$$b = \frac{1}{2} \left(\left\lceil \frac{y}{r\sqrt{3}} \right\rceil + \left\lceil \frac{y}{r\sqrt{3}} + \frac{1}{2} \right\rceil \right).$$

Here a is the number of hexagons in the direction A to B (i.e. along the long edge of the rectangle) and b is the average number of hexagons in the direction A to D (i.e. along the short edge of the rectangle). In the expression b , the two terms may differ only by one. Depending on a , there is at most a possible counting error of one hexagon. It is possible to give a formula providing the exact number of hexagons but it is not a simple expression as this one. The calculation of b is very similar to the calculation for the square tessellation in the direction of minor axis. For the calculation of a we need to use properties of hexagons. If we consider the centers of the hexagons and their projections to the line AB , the distance between two projected centers is $3r/2$. Since the distance between A and the projection of the center of the hexagon which passes through A is $r/2$, we need to subtract it from x (See Fig. 5). Therefore we can count the number of hexagons in the direction of AB by dividing $x - r/2$ by $3r/2$.

The distances between the two centers of the discs in the square and hexagon tessellations are $r\sqrt{2}$ and $r\sqrt{3}$ respectively. Therefore, the total distances travelled by the drone are approximately

$$D_S \approx \frac{xy}{r\sqrt{2}} + x + 2y + r\sqrt{2}$$

and

$$D_H \approx \frac{2xy}{3r} + \frac{2x}{\sqrt{3}} + \frac{4y}{3} + \frac{4r}{\sqrt{3}}$$

D_S denotes the length of the coverage path when the region is covered with square tessellation and D_H denotes the length of the coverage path when the region is covered with hexagonal tessellation (i.e. the length of the Hamiltonian circuit). The main terms of D_S and D_H agree with the estimates in the proof of Lemma 1. We can see that the numbers are directly proportional to the area of the region and inversely proportional to the radius of the viewing cone of the camera.

When the region is tessellated with squares, there are mainly two possible coverage paths: zigzag and spiral. The above distance estimate D_S is valid in both cases. That is, the length of a spiral path is approximately the same as the length of a zigzag path. The coverage path generated through hexagonal tessellation is shorter than the spiral and the zigzag coverage paths (See Fig. 3 and Fig. 6).

For our purposes we assume that the radius of the viewing cone of the camera is $r = 10$ and $x, y \geq 30$. Note that if either $x < 30$ or $y < 30$ then the region is very narrow which is not feasible for an analysis. In this case the back-and-forth motion may end up covering the region twice in order to return to the launch location.

By analyzing the function $D_S - D_H$ numerically we conclude that $D_S > D_H$. That is, the distance travelled by the robot is smaller in case of an hexagonal tessellation of the region. For small sized regions where $x, y < 30$, the length of the coverage path is not significantly affected by the tessellation choice.

TABLE I
COMPARISON OF SQUARE AND HEXAGON TESSELLATIONS

200 by 100	Number of captured images	Total distance
Square	120	1821m
Hexagon	98	1721m
260 by 110	Number of captured images	Total distance
Square	152	2516m
Hexagon	133	2377m

By comparing the total distances and the number of images captured (an image is captured at the center points of the polygons), the coverage obtained by a hexagon tessellation is better than the square tessellation (both for zigzag and spiral motion). Let us consider two rectangular regions, R_1 and R_2 . R_1 has a size of $x = 200m$ by $y = 100m$ and R_2 has a size of $x = 260m$ by $y = 110m$. For a camera field of view disc of radius $r = 10$, comparisons for these two rectangular regions are given in Table I. We observe that a drone which can fly 2400m on a single charge completes the coverage of the region R_2 by using the hexagon tessellation while it cannot be completed using the square tessellation.

For a scenario where a drone is supposed to perform a high altitude general survey of a region, the camera field of view disc radius will increase. Suppose $r = 20$. A square region with a side length of 230 meters can be covered with

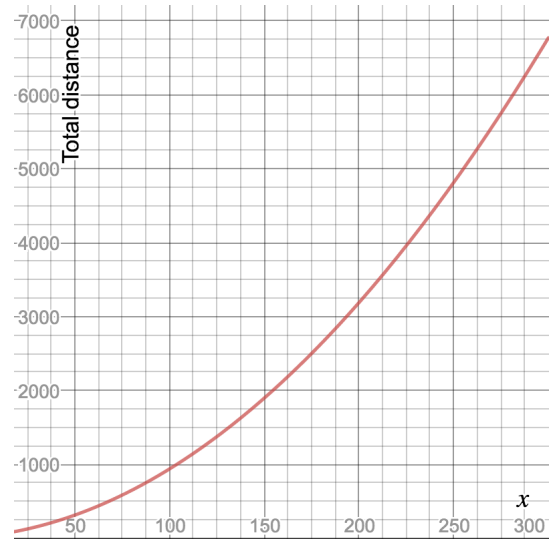


Fig. 4. The graph of D_H , the length of the Hamiltonian circuit for hexagonal tessellation, versus the side length of a square region to be covered.

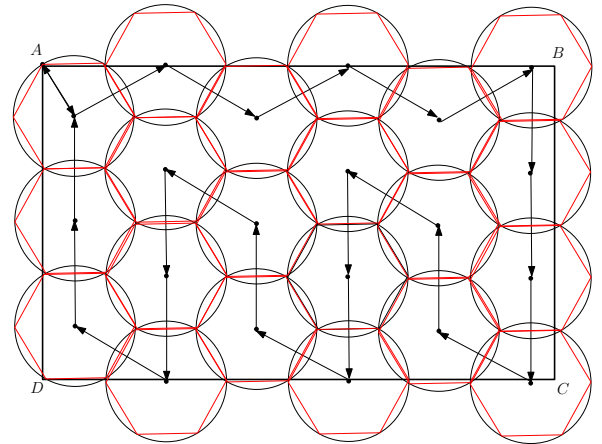


Fig. 5. Coverage by hexagonal tessellation. The Hamiltonian circuit that starts from A is also shown through arrows.

a hexagonal tessellation which creates a coverage path of length 2400 meters. Whereas, the coverage path length of the same region with a square tessellation is 2608 meters. The region can be covered by the drone on a single charge when the path is generated using hexagonal tessellation but it cannot be completed using the zigzag coverage path from the square tessellation. As the area of the target region increases the size of the extra area that can be covered through hexagonal tessellation increases.

In Fig. 4 we show the graph of the D_H for a square region with a side length of x (for $r = 10$). The graph is a parabola as we expected. Our drone which can travel a maximum distance of 2400m on a single charge can cover a square region of $171m \times 171m = 29241m^2$.

A. Hamiltonian Circuit Algorithm

A Hamiltonian path is a path on a graph that visits each vertex exactly once and a Hamiltonian circuit is a Hamiltonian path that is a cycle.

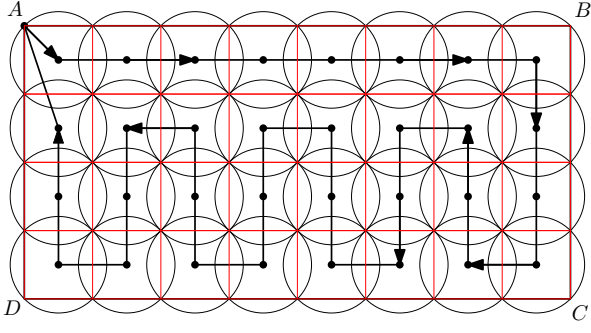


Fig. 6. Coverage by square tessellation with a zigzag path. The coverage path that starts and ends at A is shown.

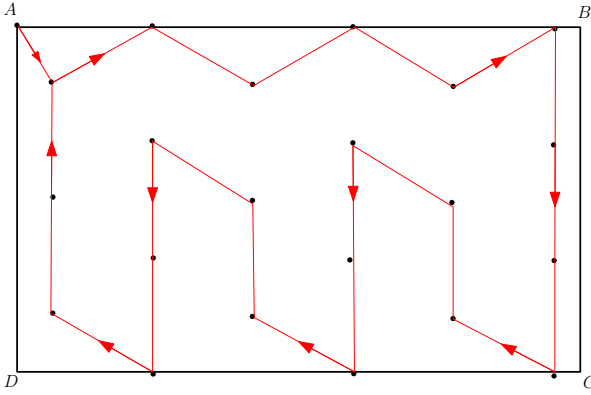


Fig. 7. Coverage path created by the Hamiltonian circuit algorithm.

In this section we provide an algorithm which outputs a Hamiltonian circuit when a hexagonal tessellation of a rectangle is given as input. The input consists of the centers of the hexagons. The algorithm will output the UAV coverage path as an ordered set of waypoints.

Let $ABCD$ be a rectangle. Whenever a hexagonal tessellation with a fixed size is given we are interested in the graph consisting of the centers of the hexagons (i.e. the centers of the circles enclosing hexagons). As described before, a tessellation can be found uniquely if the position of one hexagon is fixed. Assume that one vertex of a hexagon is aligned with A and one edge of it is on $|AB|$. In this particular tessellation we can label the centers as follows: If we consider the centers in A to D direction (i.e. along the minor axis) they will be on the same lines which are parallel to each other. We call them columns. Starting from the AB side to CD side we can label elements as 1, 2, 3, etc. This gives us row numbers. We use (i, j) to denote the center on i th element on j th column. The Algorithm 1 provides a Hamiltonian circuit as an output when a set of centers is given. An example coverage path created by the Hamiltonian circuit algorithm is shown in 7.

Algorithm 1: Hamiltonian Circuit

Input : Set of centers $\{(i, j)\}$
Output: Hamiltonian circuit: HC

```

1  $HC = [(1, 1)]$ 
2 Add 1st row (in the increasing column number) to  $HC$ 
3 Add columns to  $HC$  from the last column to 3rd column
4 if Last element of  $HC$  is  $(2, 3)$  then
5   | add 2nd and 1st column to  $HC$  in order;
6 else
7   | add centers in 1st and 2nd columns in alternating order;
8 end
```

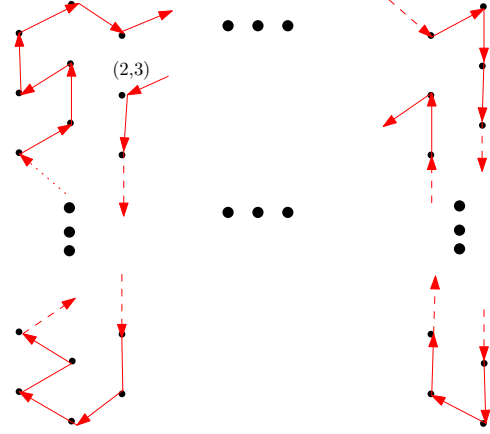


Fig. 8. A Hamiltonian circuit

In the last part of the Algorithm 1 if the last element in the list is $(2, 3)$ then we continue as previous steps (see Figure 5). If it is not the case then we need to add centers in 1st and 2nd columns alternatingly as shown in Figure 8.

The Hamiltonian circuit, which is the coverage path, for hexagonal tessellation is shown in in Fig.5 and the coverage path for square tessellation is shown in Fig.6. For square tessellation, it should be reminded that this roughly corresponds to the classical zigzag (back-and-forth motion) coverage. In this case, we modified the path after the first one along the major axis such that it goes back-and-forth along the minor axis. This is done in order to shorten the path to the launch location in the end. In most zigzag coverage pattern for UAVs, the motion along the major axis is preferred since this produces less number of turns than the one along the minor axis. However, this choice may lead the robot to complete its coverage at a point further away from the launch location. In this case, the robot completes the path by performing an extra motion along the line that connects its end point to the launch location, which is likely to increase the length of the coverage path. For this work, we assumed the number of rotations are less crucial than the overall length of the coverage path.

IV. CONCLUSION

In this paper, we show that a coverage path can be obtained by using polygon tessellation of a given area. We also show that given a rectangular region, hexagon tessellation gives a smaller number of polygons than a square tessellation. We use this result to compute a coverage path which is a Hamiltonian circuit that passes through the center points of the hexagons tiling the region and returns to the launch location. The hexagon tessellation produces a shorter coverage path than a square tessellation. Therefore, the size of the area that can be covered by a drone on a single charge is larger in the case of the path generated by hexagon tessellation than that of square tessellation. The sizes of hexagons and squares, and hence their numbers, are specified by the desired image resolution. Using this parameter, r , we can also identify the size of the region that can be covered by a drone with a single charge.

This work is mainly about finding a shorter coverage path for a UAV. However, we are still limited by the distance that can be travelled on a single charge. We have been working on the problem of efficient placement of charging stations in order to extend the area that can be covered by a drone. This is particularly useful for applications such as precision farming where the size of the field is fixed and the UAVs regularly perform tasks such as disease monitoring, fertilizer/pesticide spraying etc. which requires coverage.

Efficient placement of charging stations is one way of operating over a large area. We are also interested in extending this work to compute the coverage paths for multiple robots. The calculations and analysis performed in this work lay the foundation for the multi-robot case.

ACKNOWLEDGMENTS

The authors would like to thank Travis Henderson for providing drone flight time and camera viewing cone related parameters. This material is based upon work partially supported by the National Science Foundation through grants #CNS-1439728, #IIS-1427014, and #CNS-1531330.

REFERENCES

- [1] H. Choset, "Coverage for robotics: A survey of recent results," *Annals of mathematics and artificial intelligence*, pp. 113–126, 2001. [Online]. Available: <http://link.springer.com/article/10.1023/A:1016639210559>
- [2] E. Galceran and M. Carreras, "A survey on coverage path planning for robotics," *Robotics and Autonomous Systems*, vol. 61, no. 12, pp. 1258–1276, 2013.
- [3] T. M. Cabreira, L. B. Brisolara, and P. R. Ferreira Jr., "Survey on coverage path planning with unmanned aerial vehicles," *Drones*, vol. 3, no. 1, 2019. [Online]. Available: <http://www.mdpi.com/2504-446X/3/1/4>
- [4] E. Semsch, M. Jakob, D. Pavlíček, and M. Pechoucek, "Autonomous UAV surveillance in complex urban environments," in *Proceedings of the 2009 IEEE/WIC/ACM International Conference on Intelligent Agent Technology, IAT 2009, Milan, Italy, 15-18 September 2009*, 2009, pp. 82–85. [Online]. Available: <https://doi.org/10.1109/WI-IAT.2009.132>
- [5] A. Ahmadzadeh, J. F. Keller, G. J. Pappas, A. Jadbabaie, and V. Kumar, "An optimization-based approach to time-critical cooperative surveillance and coverage with uavs," in *Experimental Robotics, The 10th International Symposium on Experimental Robotics [ISER '06, July 6-10, 2006, Rio de Janeiro, Brazil]*, 2006, pp. 491–500. [Online]. Available: https://doi.org/10.1007/978-3-540-77457-0_46
- [6] M. Silvagni, A. Tonoli, E. Zenerino, and M. Chiaberge, "Multipurpose uav for search and rescue operations in mountain avalanche events," *Geomatics, Natural Hazards and Risk*, pp. 1–16, 10 2016.
- [7] I. Maza and A. Ollero, "Multiple uav cooperative searching operation using polygon area decomposition and efficient coverage algorithms," in *Distributed Autonomous Robotic Systems 6*, R. Alami, R. Chatila, and H. Asama, Eds. Tokyo: Springer Japan, 2007, pp. 221–230.
- [8] T. Oksanen and A. Visala, "Coverage path planning algorithms for agricultural field machines," *J. Field Robotics*, vol. 26, pp. 651–668, 08 2009.
- [9] J. Jin and L. Tang, "Coverage path planning on three-dimensional terrain for arable farming," *J. Field Robot.*, vol. 28, no. 3, pp. 424–440, May 2011. [Online]. Available: <http://dx.doi.org/10.1002/rob.20388>
- [10] D. Mitchell, M. Corah, N. Chakraborty, K. Sycara, and N. Michael, "Multi-robot long-term persistent coverage with fuel constrained robots," *Proceedings - IEEE International Conference on Robotics and Automation*, vol. 2015-June, no. June, pp. 1093–1099, 2015.
- [11] C. Di Franco and G. Buttazzo, "Energy-aware coverage path planning of UAVs," *Proceedings - 2015 IEEE International Conference on Autonomous Robot Systems and Competitions, ICARSC 2015*, pp. 111–117, 2015.
- [12] T. M. Cabreira, C. D. Franco, P. R. Ferreira, and G. C. Buttazzo, "Energy-Aware Spiral Coverage Path Planning for UAV Photogrammetric Applications," *IEEE Robotics and Automation Letters*, vol. 3, no. 4, pp. 3662–3668, 2018.
- [13] C. Di Franco and G. Buttazzo, "Coverage Path Planning for UAVs Photogrammetry with Energy and Resolution Constraints," *Journal of Intelligent and Robotic Systems: Theory and Applications*, vol. 83, no. 3-4, pp. 445–462, 2016.
- [14] M. Wei and V. Isler, "Coverage path planning under the energy constraint," *2018 IEEE International Conference on Robotics and Automation (ICRA)*, pp. 368–373, 2018.
- [15] A. Xu, C. Viriyasuthee, and I. Rekleitis, "Efficient complete coverage of a known arbitrary environment with applications to aerial operations," *Auton. Robots*, vol. 36, no. 4, pp. 365–381, Apr. 2014. [Online]. Available: <http://dx.doi.org/10.1007/s10514-013-9364-x>
- [16] S. Bochkarev and S. L. Smith, "On minimizing turns in robot coverage path planning," in *CASE. IEEE*, 2016, pp. 1237–1242. [Online]. Available: <http://dblp.uni-trier.de/db/conf/case/case2016.html#BochkarevS16>
- [17] S. A. Sadat, J. Wawerla, and R. T. Vaughan, "Recursive non-uniform coverage of unknown terrains for UAVs," *IEEE International Conference on Intelligent Robots and Systems*, no. Iros, pp. 1742–1747, 2014.
- [18] S. Lim and H.-C. Bang, "Waypoint planning algorithm using cost functions for surveillance," *International Journal of Aeronautical and Space Sciences*, vol. 11, pp. 136–144, 06 2010.
- [19] C.-Y. Chang, C.-C. Chen, and C.-C. Liu, "A novel approximation algorithm for minimum geometric disk cover problem with hexagon tessellation," *Smart Innovation, Systems and Technologies*, vol. 20, pp. 157–166, 01 2013.
- [20] R. J. Fowler, M. S. Paterson, and S. L. Tanimoto, "Optimal packing and covering in the plane are np-complete," *Information Processing Letters*, vol. 12, no. 3, pp. 133 – 137, 1981. [Online]. Available: <http://www.sciencedirect.com/science/article/pii/0020019081901113>
- [21] D. S. Johnson, "The np-completeness column: An ongoing guide," *Journal of Algorithms*, vol. 7, no. 4, pp. 584 – 601, 1986. [Online]. Available: <http://www.sciencedirect.com/science/article/pii/0196677486900209>
- [22] S. Narayanappa and P. Vojtechovsk, "An improved approximation factor for the unit disk covering problem," 01 2006.
- [23] A. Biniarz, P. Liu, A. Maheshwari, and M. Smid, "Approximation algorithms for the unit disk cover problem in 2d and 3d," *Computational Geometry*, vol. 60, 04 2016.
- [24] C.-C. Chen, C.-Y. Chang, and P.-Y. Chen, "Linear time approximation algorithms for the relay node placement problem in wireless sensor networks with hexagon tessellation," *Journal of Sensors*, vol. 2015, pp. 1–12, 05 2015.
- [25] B. Grünbaum and G. C. Shephard, "Tilings by regular polygons," *Mathematics Magazine*, vol. 50, no. 5, pp. 227–247, 1977. [Online]. Available: <http://www.jstor.org/stable/2689529>